

## *Final report*

### **Main goals of the project**

The ultimate goal of the project has been to understand the biological role of the endogenous single-strand discontinuities, nicks, discovered by our group in nonapoptotic, live cells from yeast to human systems earlier (1-7). These earlier data also suggested that these nicks delimit loop-size chromatin regions, are juxtaposed with RNA/DNA-hybrids (1) and may serve as anchorage sites of superhelical chromatin loops.

### **Complexities, intricacies, challenges**

To clarify the possible role of the nicks observed, and especially the molecular mechanisms involved in their generation, has proved difficult for two main general reasons. On the one hand, there are several, crucial, but divergent questions that all urge for interpretation, since they all raise issues of critical importance regarding the discontinuities themselves. For example, mapping of nicks along the chromosomes is technically possible (accomplished in this project, see below), yet the question where nicks are localized relative to supercoiled domains (having no nicks at all, by definition), is a question that, without tackling this aspect as well, would raise serious doubts about the whole project. On the other hand, localization of the nicks and R-loop accumulation to the promoter and terminator regions of the genes (see our results below) raises questions regarding the relationship of transcriptional activity to the supercoiled state, a fundamental issue on its own, requiring additional studies. So, we have been forced, and also allured, to follow a rather broad approach that has eventually led us to propose a model of higher-order chromatin organization within the cell nucleus of wider significance, compared to our original program; see „Overall conclusions...”, below. Second, the enzymatic assays used by us to detect nicks rely on enzymatic reactions which are complex (DNA polymerases share not only exonuclease, but also RNase H activity, they can misincorporate and also elongate ribonucleotides, with topoisomerase I being recruited to the sites of misincorporated ribonucleotides, leaving a labile cyclic nucleotide here, what eventually becomes healed via the transient formation of a nick (8)). Knowing exactly our other main tool, an monoclonal antibody specific for RNA/DNA-hybrids, also demanded lots of background work involving the detailed characterization of its specificity, to a degree highly exceeding the amount of data available on the issue through published information: There haven't been unambiguous data on the size of the hybrids recognized by the antibody, a question crucial for interpretation of the cytological pictures, nor was it certain if what we see are indeed R-loops rather than one or another from among the different non-B nucleic acid structures of different significance. Moreover, based on topoisomerase I – related literature, R-loops may also be generated as a result of superhelical changes ensuing upon deproteinization (see e.g. ref. 9), when the equilibrium maintained by the nucleosomal

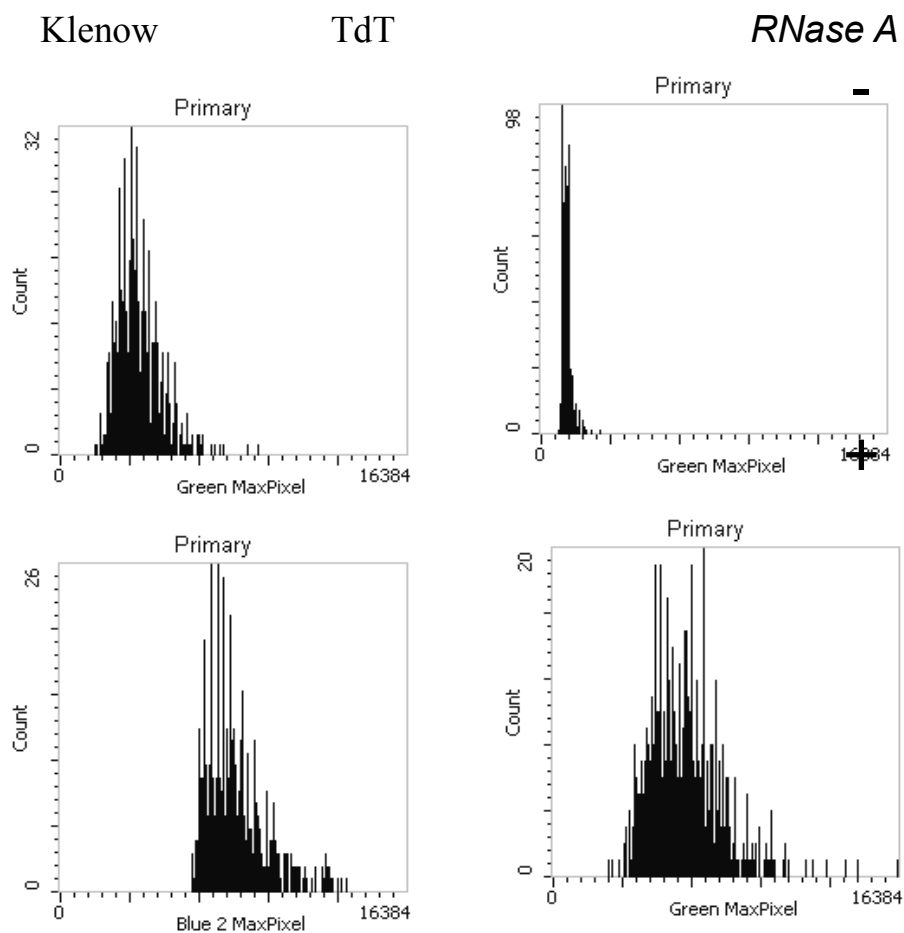
structure abruptly changes the earlier relationship between twist and writhe; thus we had to convince ourselves that the R-loops detected in our systems emerge and exist in vivo. Additionally, mapping of single-strand breaks has proved a challenging technical task, making development of new strategies necessary.

### **Overall conclusions based on the work accomplished in the context of this OTKA project**

Our present view of how the linear chromatin structure and nuclear architecture are coupled to each-other to form the higher-order levels of the structural hierarchy thought to characterize overall chromatin structure is based on data obtained for particular loci rather than on approaches interrogating the global genome. We have shown that genomic sites enriched in transcription dependent R-loops are specifically recognized both by an RNA/DNA-specific antibody and also by nick-labeling at these sites. R-loops are enriched at the promoters and terminator sequences of genes both in yeast and human cells. These sites that are localized in the nuclear periphery, underneath the lamina, are bona fide anchorage points delimiting chromatin loops in view of the fact that the DNA between them is supercoiled, as demonstrated in nuclear halos. Incorporation of nucleotides proceed at these sites in both transcription and replication. These observations allow us to envision the nuclear architecture with transcriptional activity involving the formation of R-loops being organized via anchoring the two ends of the genes to the nuclear matrix, a structure identical or associated with the lamina.

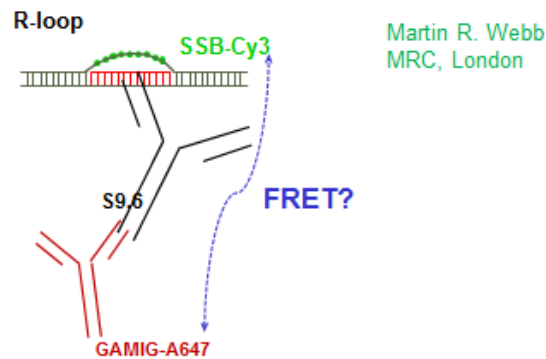
In our work performed with the support of this OTKA grant we have reached the following **Specific conclusions (1-28) below:**

1. We have confirmed by terminal deoxynucleotidyl transferase (TdT) labeling that nicks with free 3'OH are juxtaposed with and masked by RNA structures that are sensitive to RNase A (and H1) digestion. We have also confirmed our earlier results (1) by quantitative laser scanning cytometry (LSC) that labeling by Klenow enzyme becomes possible only after RNase digestion. Since labeling efficiency of RNA by TdT is very low, and we have a great increase in labeling after RNases, the template / substrate of the polymerization reaction must be DNA.

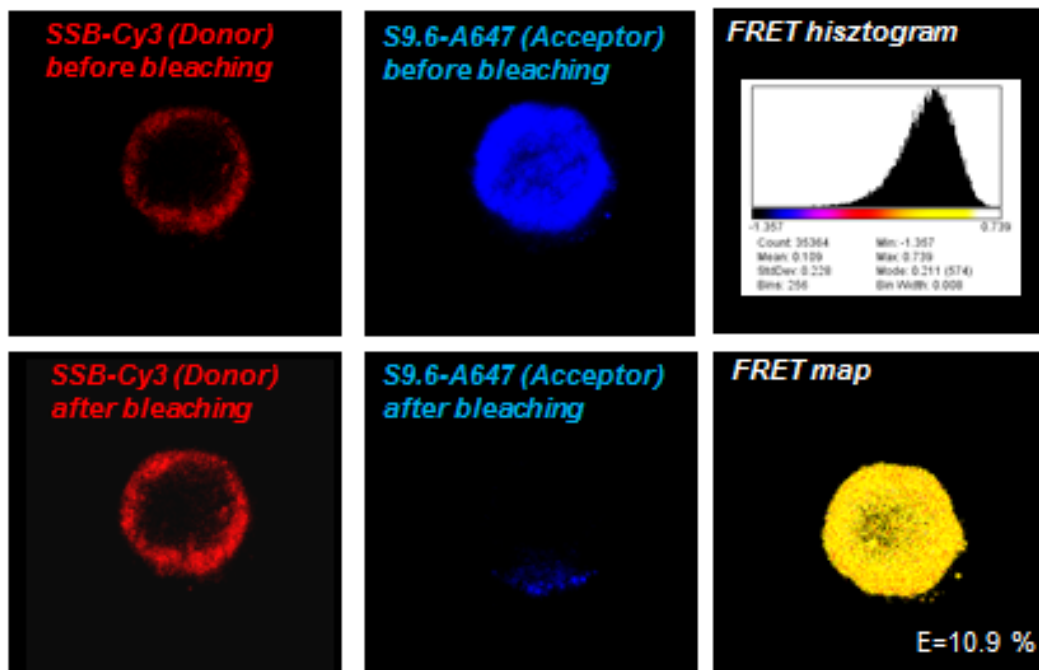


- The RNA/DNA-hybrids comprise R-loops, based on acceptor photobleaching FRET between Cy3-labeled single-strand binding protein (SSBP; obtained from M. R. Webb, London) and the hybrid-specific antibody, S9.6 (ATCC).

Molecular co-localization by FRET of RNA/DNA-hybrids and ss DNA regions

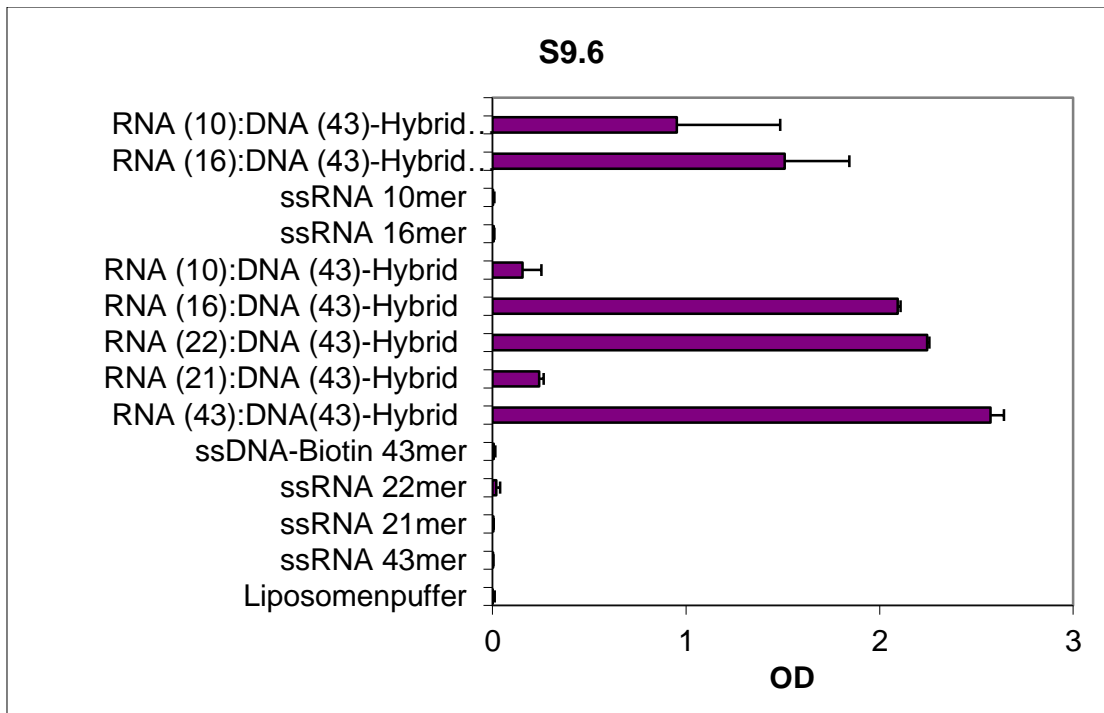


**ssDNA** and **RNA-DNA hybrids** are in molecular proximity  
Acceptor-photobleaching FRET



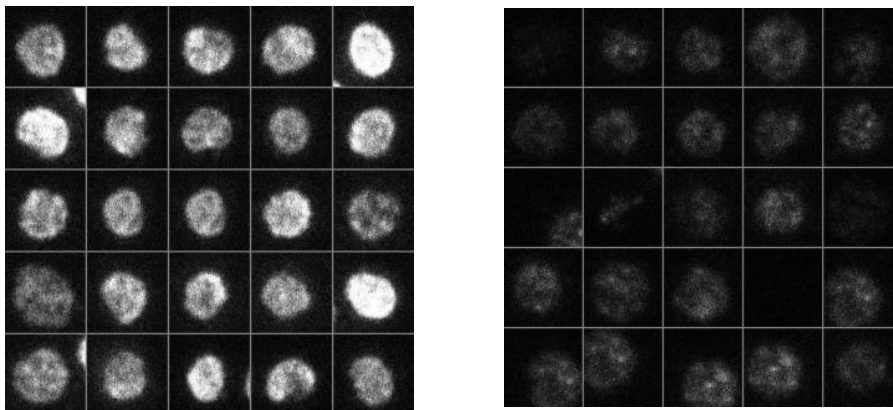
➡ **RNA/DNA-hybrids are R-loops**

3. The specificity of this antibody was further investigated by ELISA (in collaboration with S. Bauer, Marburg); these data show that S9.6 can specifically bind to hybrids as short as 10 bp, i.e. R-loops, what may also be formed within the regions covered by RNA polymerase upon deproteinization.

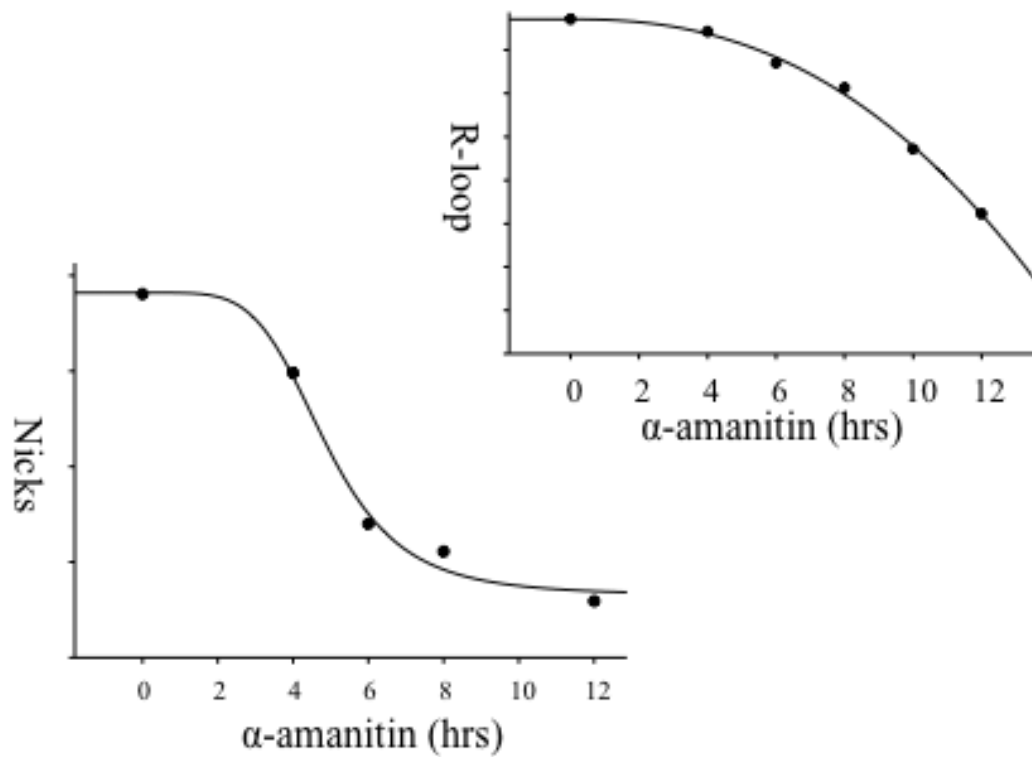


4. The specificity of this antibody was confirmed using specimen of fixed cells on slides, by its competition with recombinant catalytic site mutant RNase H1 (obtained from S. Kanaya, Osaka).

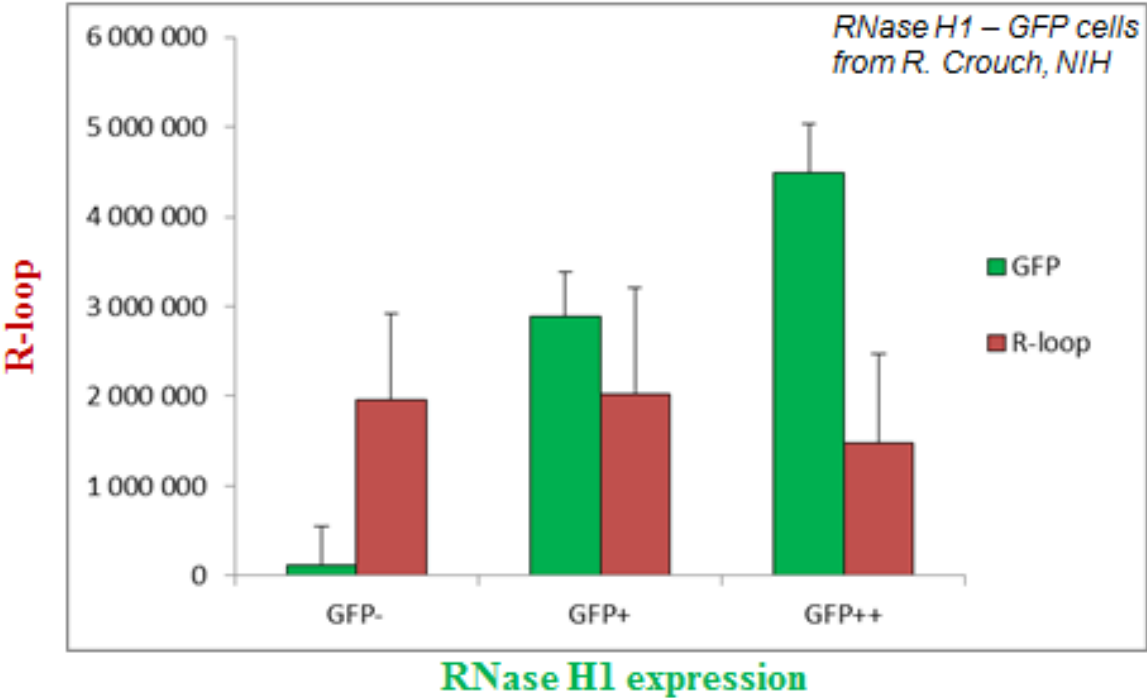
RNaseH D135A-> Fix-> S9.6-> GAMIG-A647:



5. Both the level of R-loops, detected by S9.6, and the incidence of nicks, detected by in situ nick translation, are sensitive to transcription inhibition, e.g. by alfa-amanitin, albeit exhibiting different kinetics of response.

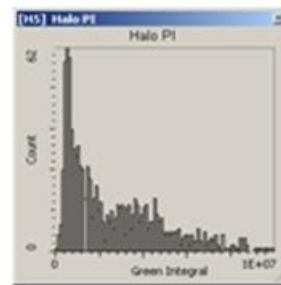
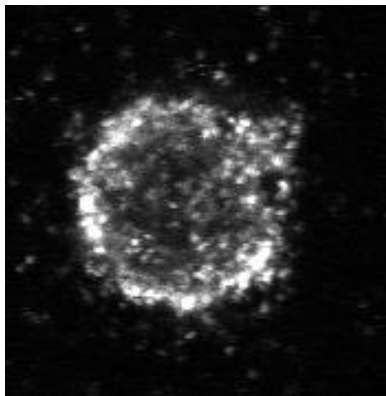


The R-loops detected by the S9.6 antibody at least partly arise de novo, rather than upon sample preparation, since expression of RNase H1-GFP (obtained from R. Crouch, NIH, Bethesda, USA) inversely correlates with S9.6 labeling intensity in these nuclei.



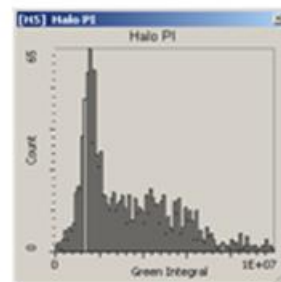
6. The nicks are localized to the periphery of the nuclei, underneath the nuclear lamina, when visualized by nick translation including terminator nucleotides among the triphosphates to limit labeling to the vicinity of the endogenous nicks, and appear to be topoisomerase dependent. (The ratio of dideoxynucleotides was optimized using our rDNA system; see below)

The left picture shows the result of nick-translation performed by *E. coli* DNA polymerase I in the presence of dideoxynucleotides on an agarose-embedded nuclear halo sample (of human Jurkat cells). The right panel shows that labeling by DNA polymerase I, although decreases, still essentially withstands prior RNase treatment, confirming that it is DNA (rather than RNA) what becomes labeled. The lower panel demonstrates that in MCF7 cells with constitutively silenced topoisomerase I gene the average intensity of nick-labeling, i.e. number of nick-containing sites in view of the protocol including terminator nucleotides, when normalized on DNA content, is decreased upon topoisomerase silencing. In this experiment the two kinds of differentially labeled cells were mixed in one chamber and measured together, to make comparison accurate.

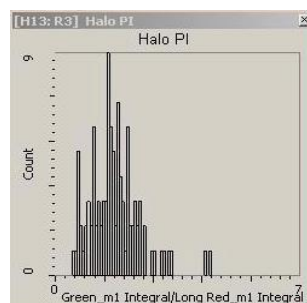


RNaseA

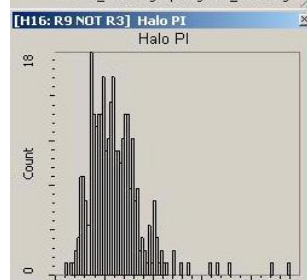
+



-



MCF7

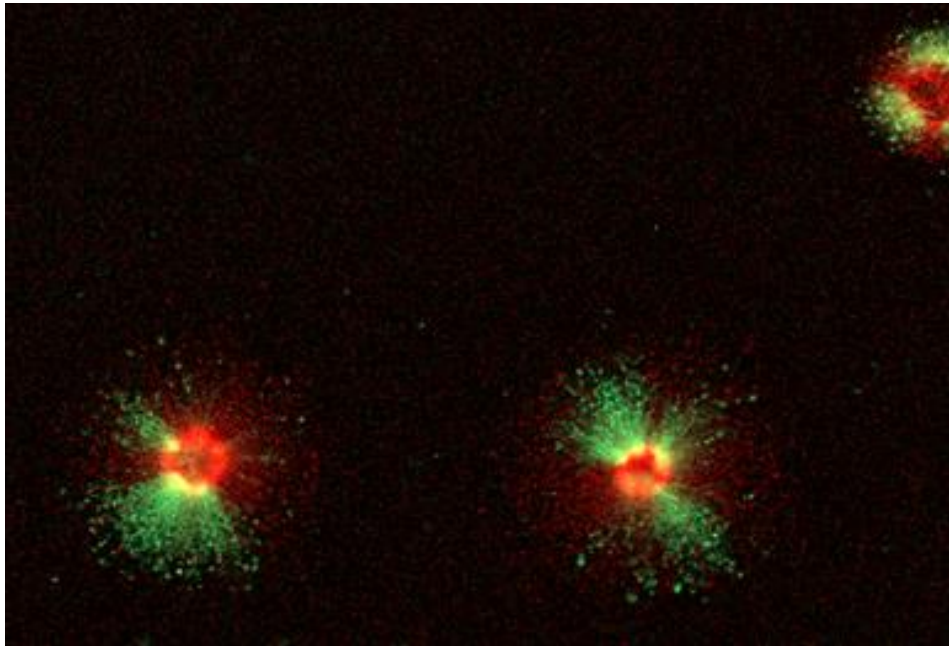


MCF7top1s

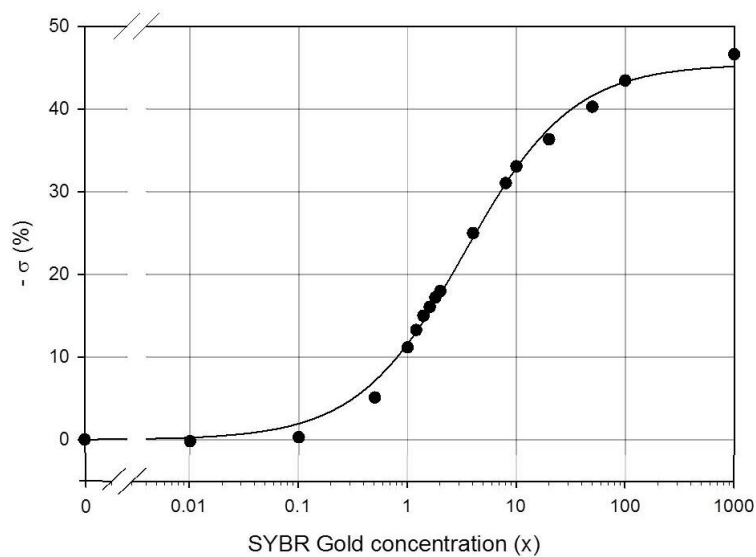
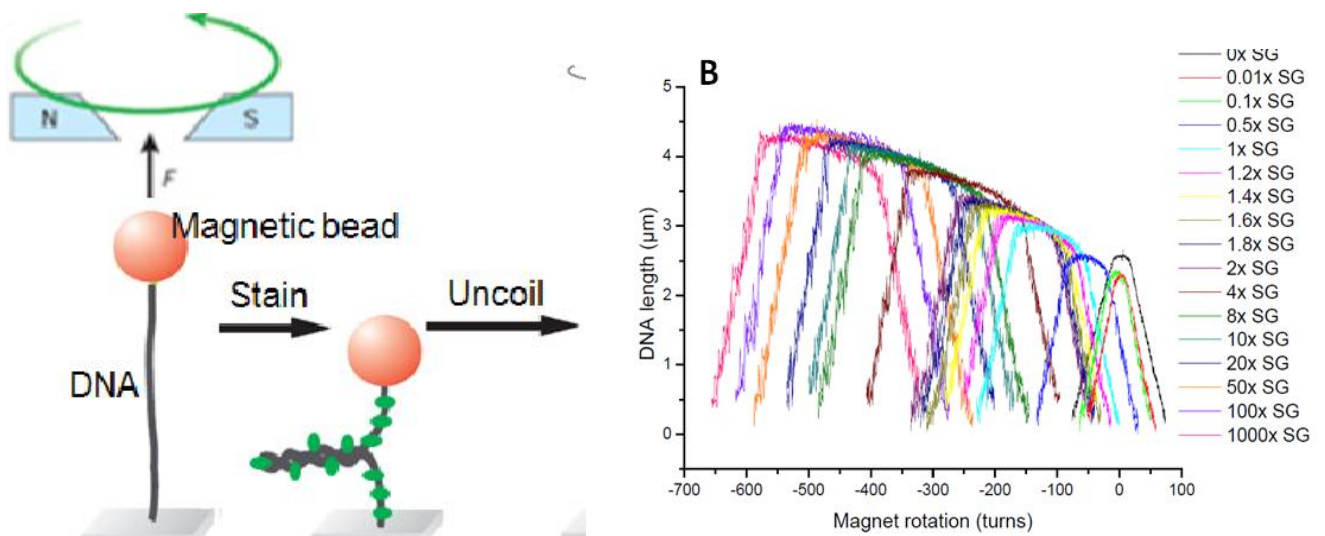


7. We have observed that the nicks and the supercoiled loops occupy different topological domains (see also below). This conclusion relies largely on the assumption that the experimental system, of nuclear halos, preserves much of the in vivo characteristics of higher order chromatin architecture. The result below, and those under 8-11, support this assumption.

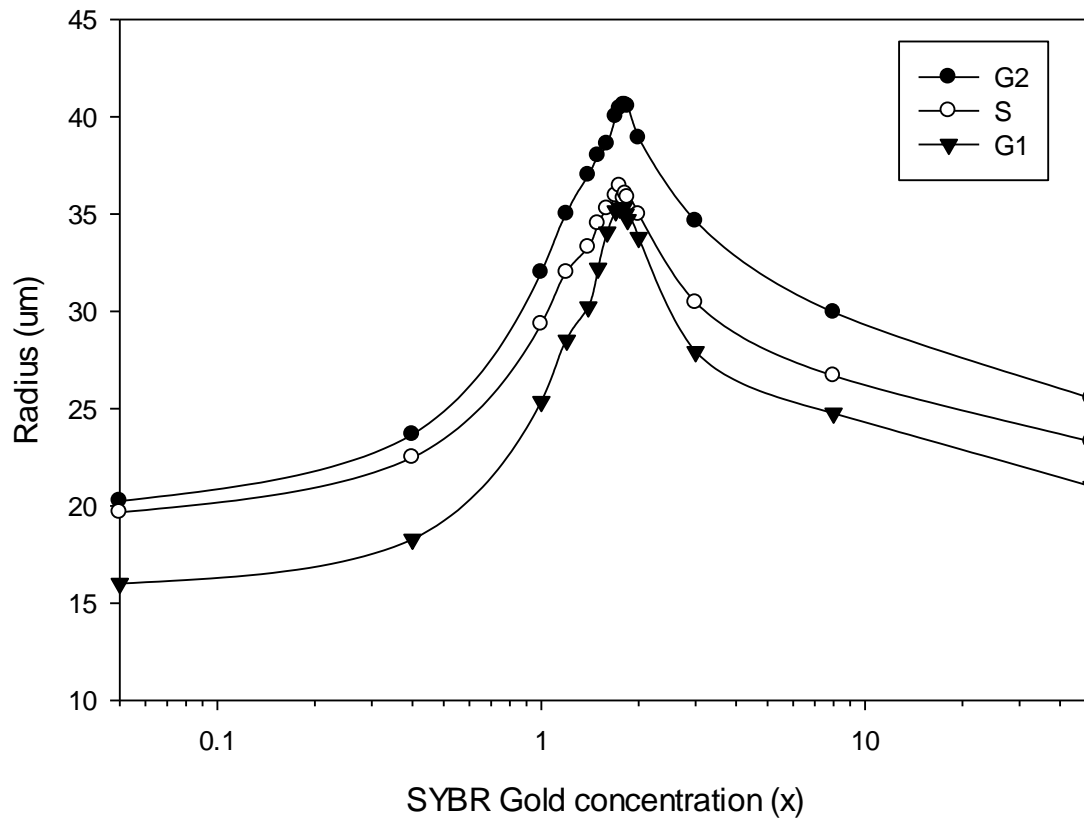
After pulse-labeling with BrdU, following several rounds of cell division, chromosomes randomly lose their original labeling in a yes-or-no fashion, due to the semiconservative nature of replication and the random segregation of sister chromatids, with the labeled chromosomes depicting distinct territories. This phenomenon is recapitulated in our halo samples, i.e. the chromosome territories are preserved well in these samples, suggesting that the halos reflect much of the original higher-order chromatin structure present inside the nucleus.



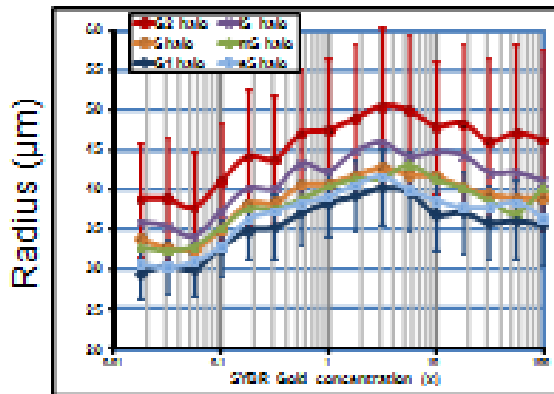
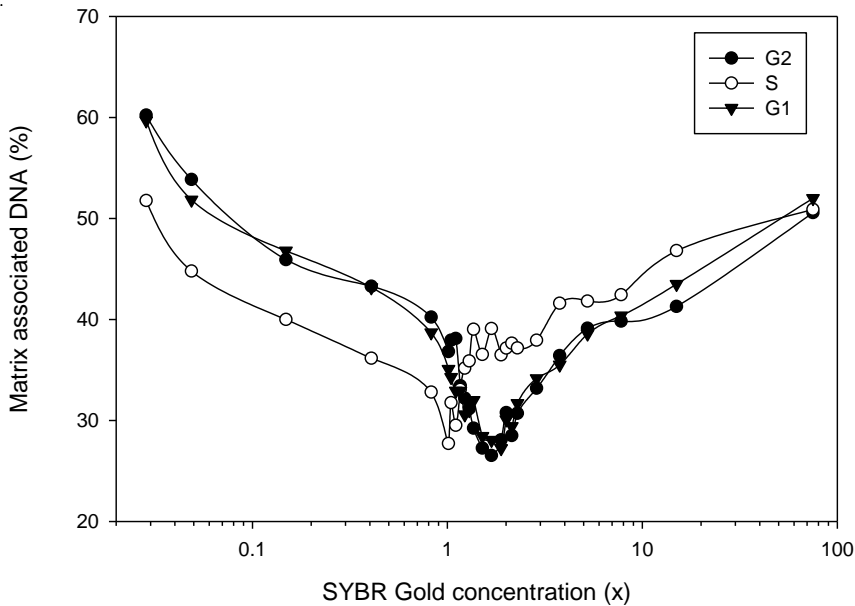
8. The degree of superhelicity of the DNA loops between the nicked regions corresponds to the level expected for the overall superhelicity estimated by others using different approaches. This is based on calibration of our winding curves with parallel single-molecule measurement of superhelicity in collaboration with R. Seidel, Muenster. Superhelical densities ( $\sigma$ ) generated by different intercalator (SYBR Gold) concentrations were calculated from the center shift values (see right figure (“B”) below) measured at different dye concentrations. Taking also nonspecific adsorption of the dye (to the nucleus, to the walls or bottom of the chamber) into account, the average superhelical density based on the free dye concentration could be calculated, and it was within (at the higher limit of, i.e. at  $\sigma \approx -12.5\%$ ) the expected range (7-12 %).



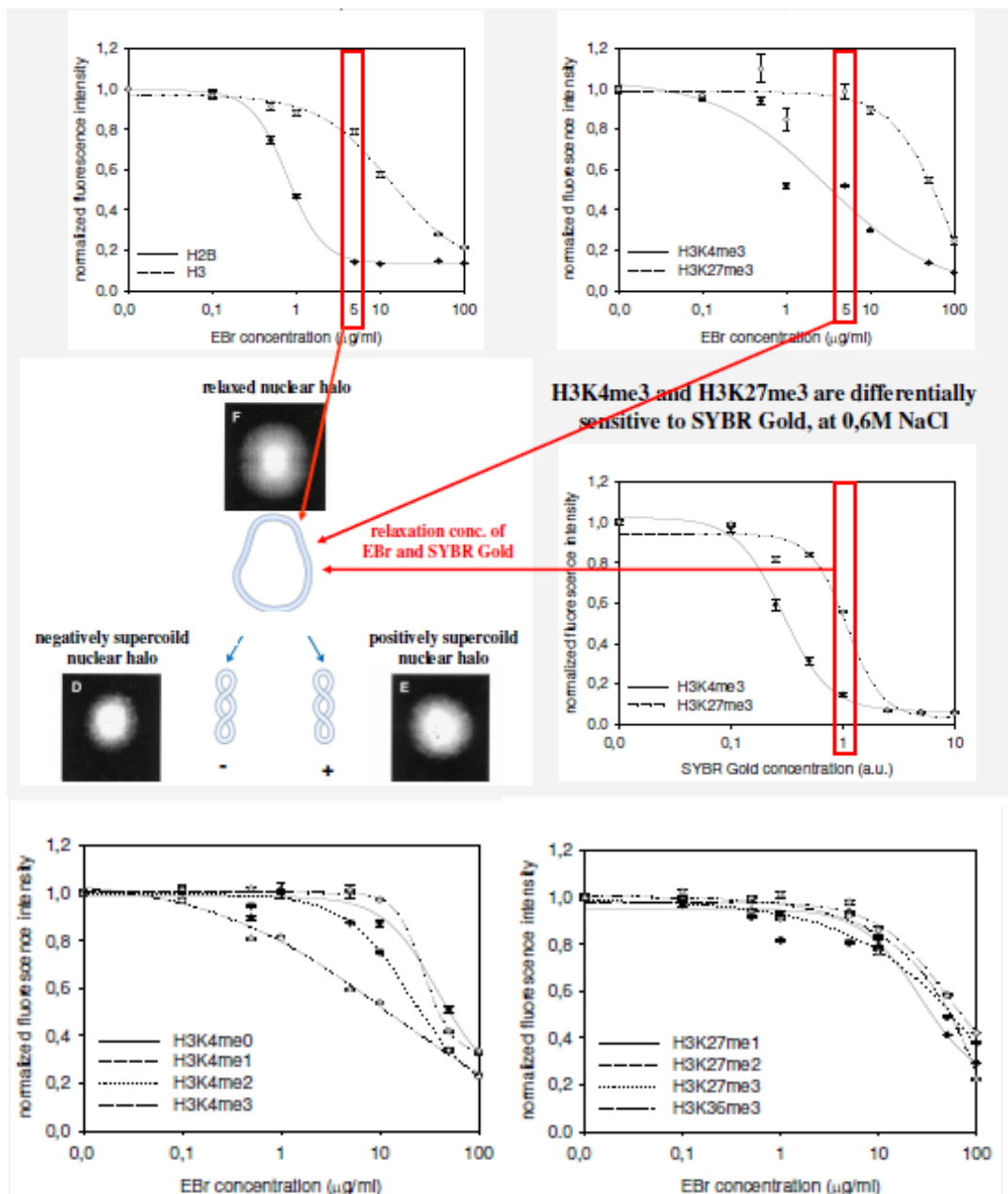
9. In the Laser Scanning Cytometric (LSC) analysis of nuclear halos used for measuring superhelicity, cell cycle phase-specific demonstration of the incidence of nicks was possible (as a result of using the high quantum yield fluorescent Sybr Gold dye), allowing us to conclude that the nicks are present in any phase of the cell cycle, i.e. they do not arise in a replication dependent manner, in S phase.



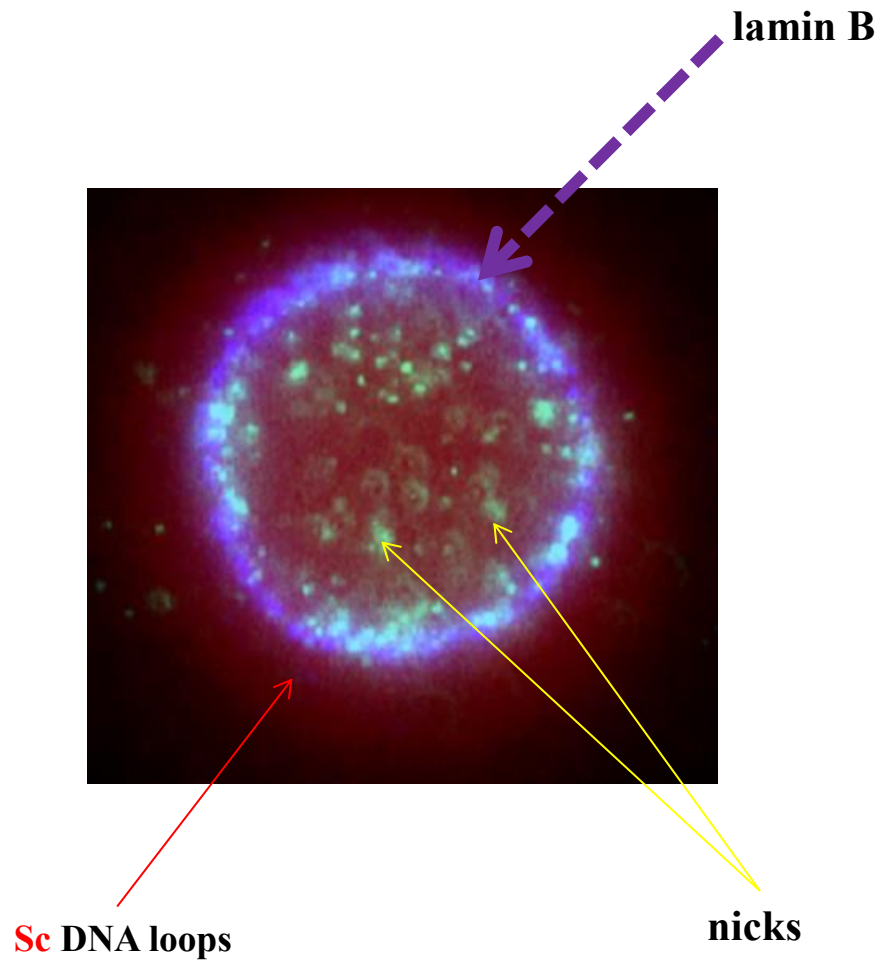
10. Matrix association of the DNA depends strongly on the superhelicity and on the cell cycle phase, as shown in the upper panel. Matrix association was calculated from the fluorescence integrals of the halo- and matrix areas at different intercalator concentrations (Jurkat cells). Therefore, and in view of a body of topoisomerase-related published data, we have checked if artificial nicks generated by UV or H<sub>2</sub>O<sub>2</sub> treatment do not become anchored to the lamina-bounded nuclear „matrix”. As shown in the lower panel, the halos remain visible and become extended, rather than overwound, upon intercalation, arguing against this possibility. Having realized that the shape of the winding curve is very sensitive to the different degrees of amplification that was necessary to use at the different intercalator (dye) concentrations, a multithreshold data analysis has been developed to correct for any amplification related artifacts.



11. Transcription and replication, at the very site of the DNA where these enzymatic reactions occur, are apparently favored by loose nucleosome-DNA binding. We asked if the nicked, i.e. relaxed state of DNA at these sites is indeed accompanied by weaker cohesion between nucleosome and DNA. Having developed a LSC-based method based on elution of histones with intercalator (or salt) treatment, we could prove that the H3K4me3 active mark carrying tetramers become less tightly attached to DNA than bulk histones or the inactive mark H3K27me3 decorated nucleosomes. In this assay, after salt and/or intercalator elicited elution of agarose-embedded isolated nuclei, the remaining histone levels are determined by immunofluorescence labeling, using a panel of modification-specific monoclonal antibodies. The elution characteristics of bulk histones were assessed by using cell lines expressing GFP-tagged H3. Significantly steeper profiles (indicating loosely bound histones) could be measured in the case of H3K4me3 and H3K27ac, in contrast with inactive marks like H3K27me1, H3K27me2, H3K27me3, H3K9me1, H3K9me2, H3K9me3 and other active marks, including H3K36me3, H3K4me0, H3K4me1, H3K4me2, H3K9ac, H3K14ac.



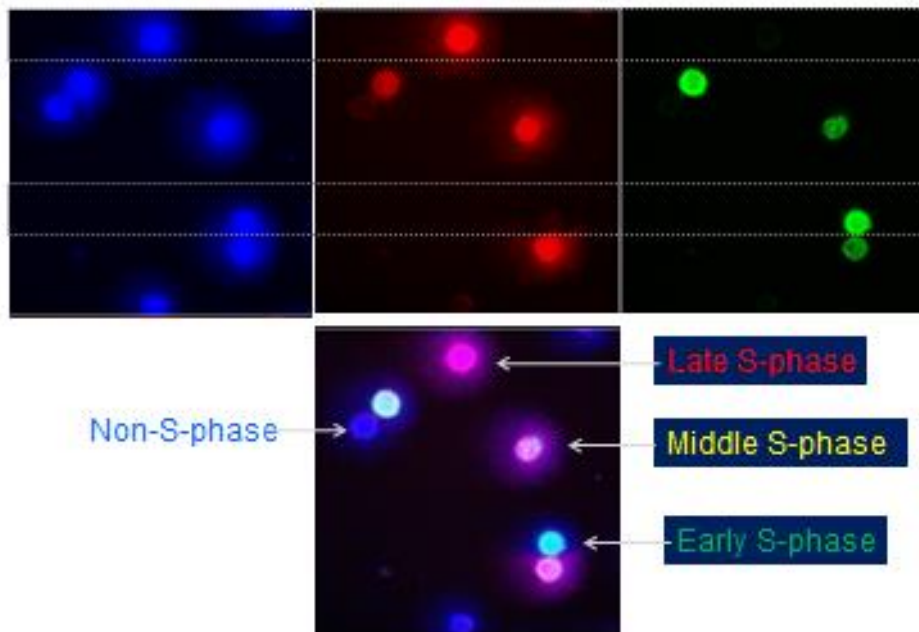
12. The above data, when considered together, allow us to suggest that the chromatin consists of two topologically separated domains: that of the supercoiled (**sc**) loops, and the nicked DNA containing „matrix”. The following two results (13, 14) let us suggest that both transcription and replication proceed in the domain where nicks occur.



13. Upon sequential labeling of the DNA during replication, using transiently permeabilized cells, we have shown that replication occurs on the „matrix” and goes out to the superhelical domain afterward.

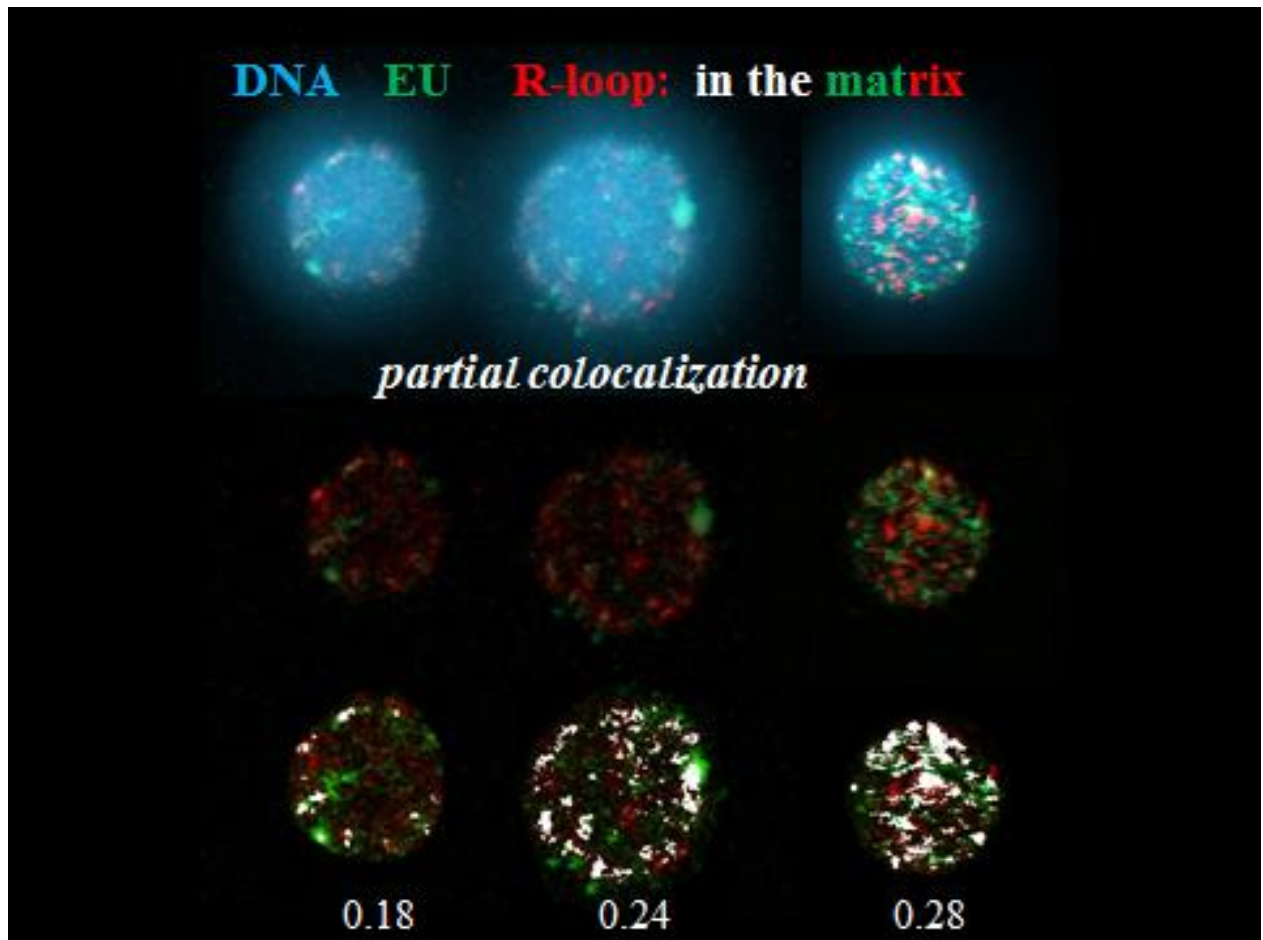
### DNA replication: *in the matrix*

DAPI pulse 1 (EdU), chase: 3 h, pulse 2 (biotin-dUTP)



Permeabilization according to: *Koberna et al. Chromosoma. 1999, 108(5)*

14. Immunolocalization of freshly transcribed RNA has shown that transcription also occurs on the „matrix”. However, the partial co-localization of freshly transcribed RNA with R-loops shows that R-loops detected by S9.6 comprise a heterogeneous group of RNA/DNA-hybrids.

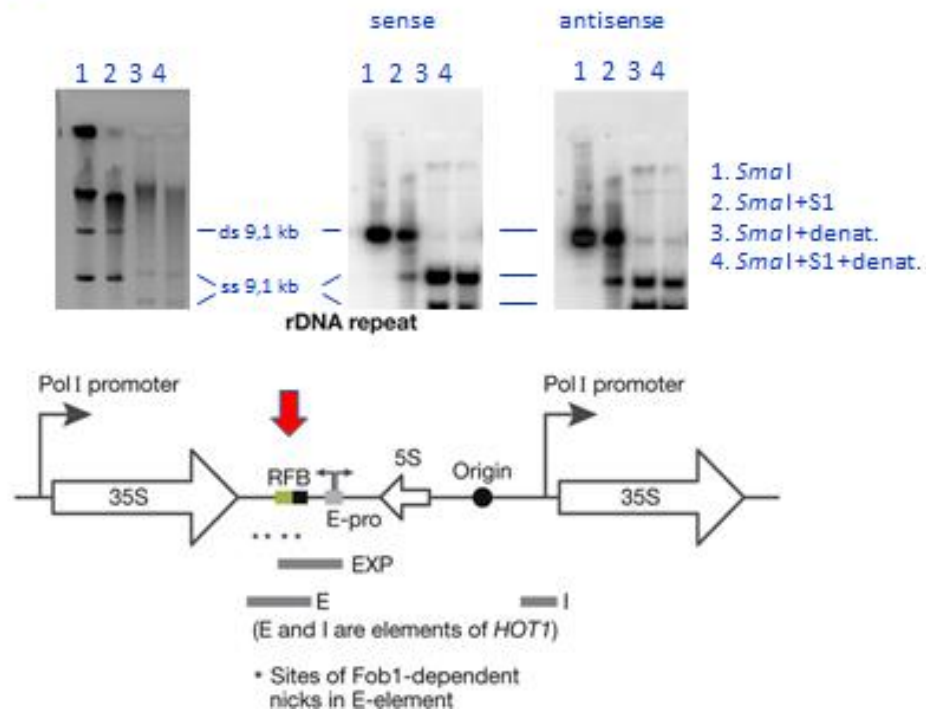




15. The planned localization studies have been completed in *S. cerevisiae*, both in the rDNA locus and on the whole genome, showing nonrandom distribution of both entities, as detailed below.

In the rDNA locus, mapping by Southern blotting proved difficult and has led to ambiguities, due to the (rarely recognized) nicking activity of many restriction endonucleases at imperfect recognition sites, making endogenous nicks hardly distinguishable. However, having developed a novel method for the purposes of strand-specific localization, we could map a non-artefactual nick, one on both strands, around the replication fork barrier (RFB). (These were not readily observed by our reverse South-Western blot (see below), probably due to their „dirty end” character, as expected for a bona fide topoisomerase I cleavable complex, known to exist at the RFB.)

### Mapping of nicks within the rDNA cluster, using urea/agarose-FIGE (Hegedus et al., NAR, 2010):



16. To enhance the sensitivity of our nick mapping, in view of the difficulties implied by the faint bands in the Southern blot experiments (above), a new procedure was developed (what has turned out to be known already as „reverse South-Western blot”), where biotinylated nucleotides are incorporated into the immediate vicinity of the nick in intact, deproteinized DNA of fixed, agarose-embedded yeast cells, to be detected after restriction digestion, electrophoresis and blotting, by immunolabeling and chemiluminescence. Quite unexpectedly, R-loops were preserved during the procedure and could be detected and mapped in an analogous fashion, using the S9.6 mAb.

## rSouth-Western blot

Cells cross-linked with HCHO



Lyticase, PK

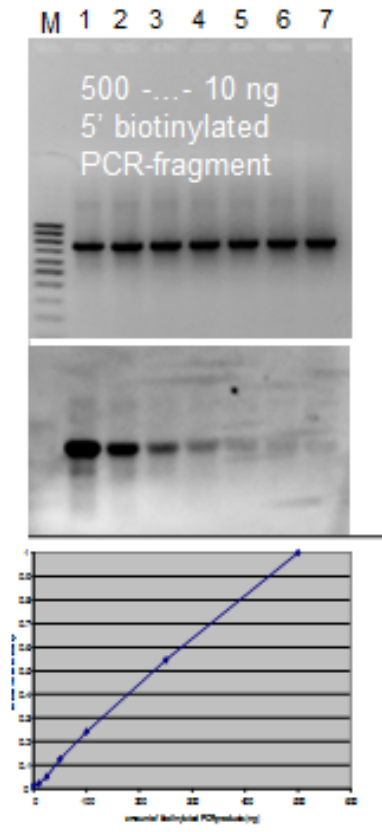
DNA Pol , biotin-dNTP + ddNTP

Cut out 9.1 kb rDNA unit, restrict.

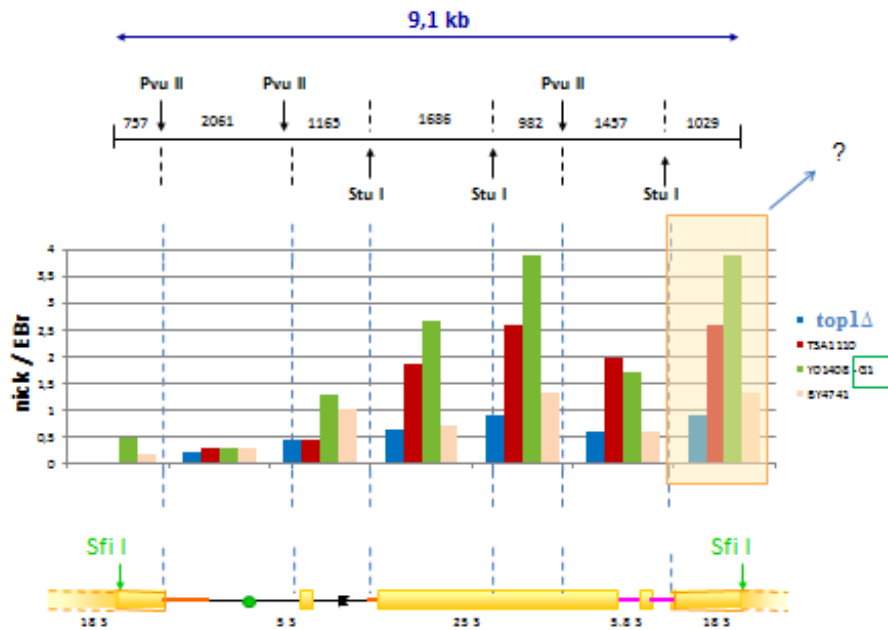
Electrophoresis

Blotting

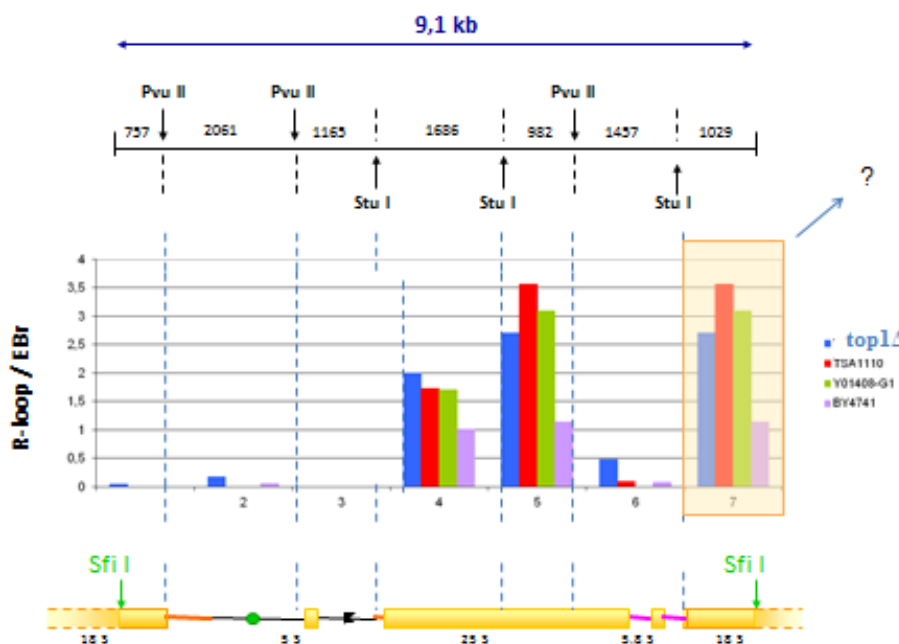
$\alpha$ -biotin or S9.6 mAbs



17. These studies have shown that both entities are enriched in the gene body of the 25S rRNA gene. (The area of the 18 S rDNA gene could not be distinguished well from a fragment of the 25 S gene; measurements in this region, using other combinations of restriction enzymes, are underway). These experiments have revealed nicks that are nick-translatable, as opposed to the Southern-blot that reveals any ss discontinuity, but which is sensitive enough to detect only site-specific nicks localized at fixed position.

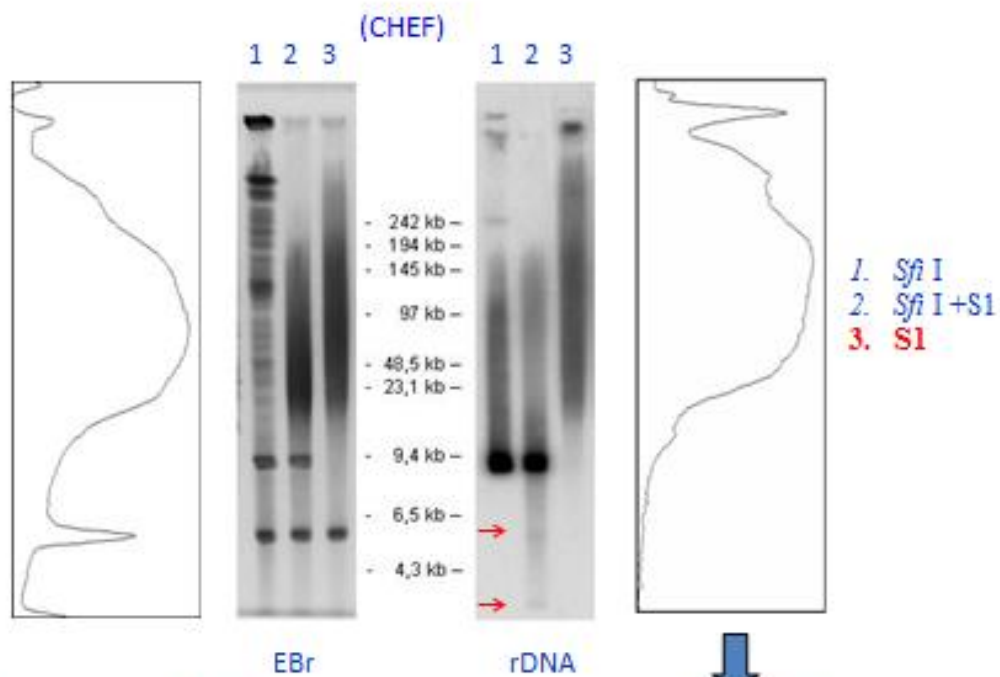


P18.



18. Southern blot analysis (using an rDNA specific probe) of the total rDNA locus has revealed that every ~5-10th rDNA 9.1 kb unit harbors the endogeneous nicks detected, suggesting that epigenetic features and chromatin function are partly responsible for the definition of the nicks. Similar conclusion was drawn when hybridizing with another probe of the rDNA repeat.

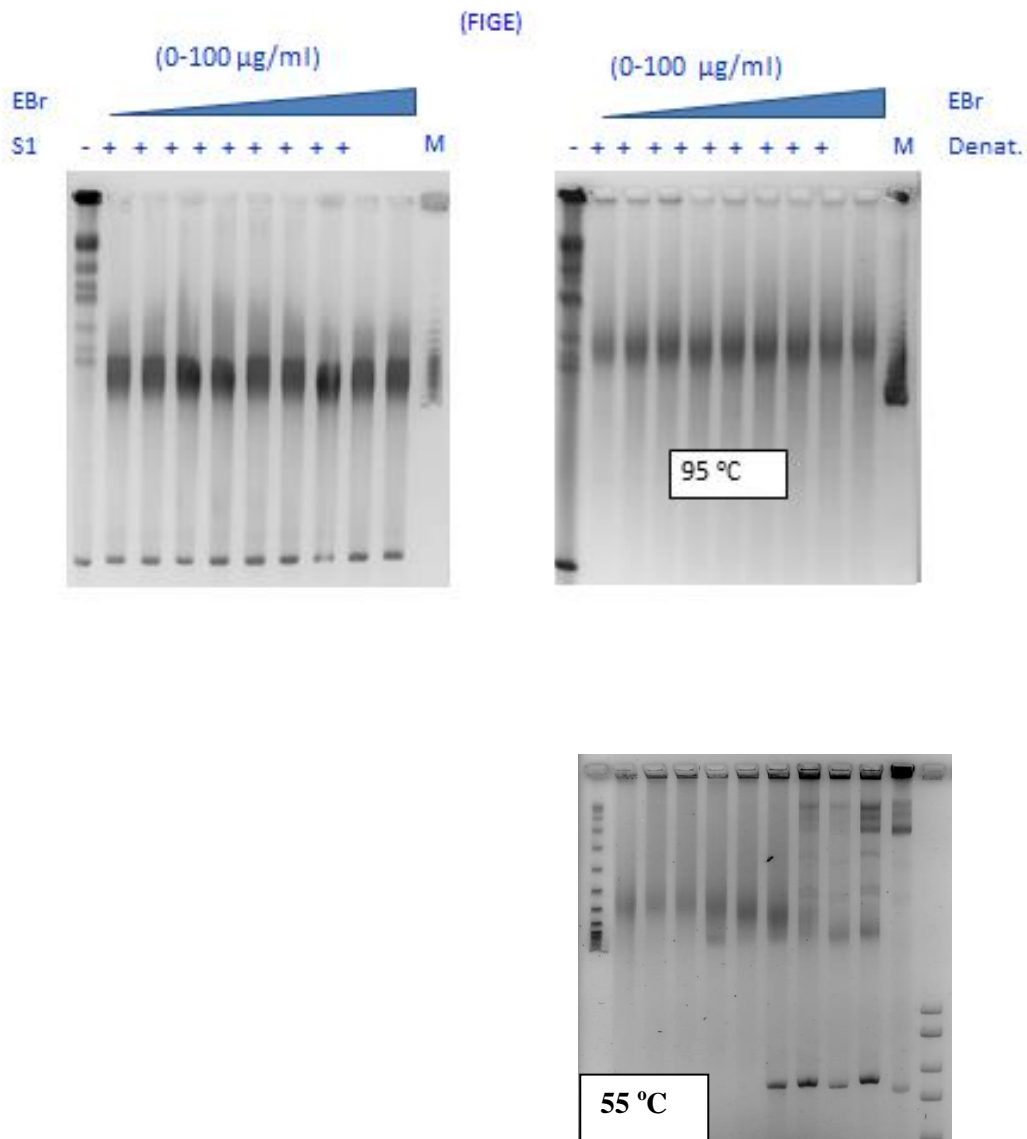
### Loop-size fragmentation within the rDNA cluster



→ nicks in every 5-10th unit

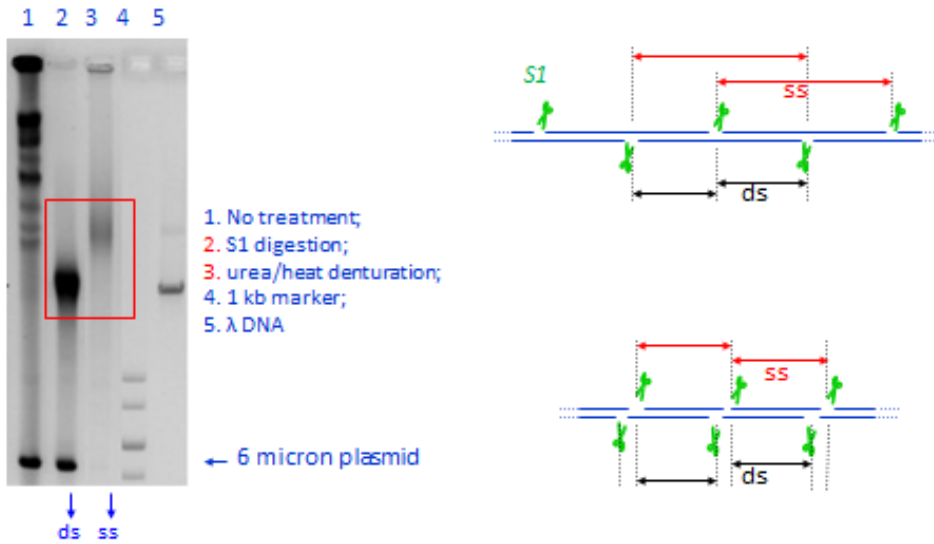
20 - 200 kb

19. The possibility that the correlation of nick incidence with loop-size is a simple consequence of a scenario where the first random nick might relax the DNA what may become resistant to any further nicking activity, was excluded in experiments where an intercalator was added to the cells prior to lysis: although the intercalator increased the melting point of the DNA present in these samples significantly (revealed at 80 °C), proving its presence, the incidence of nicks was not altered when the ss size of the fragments was compared at fully denatured state.

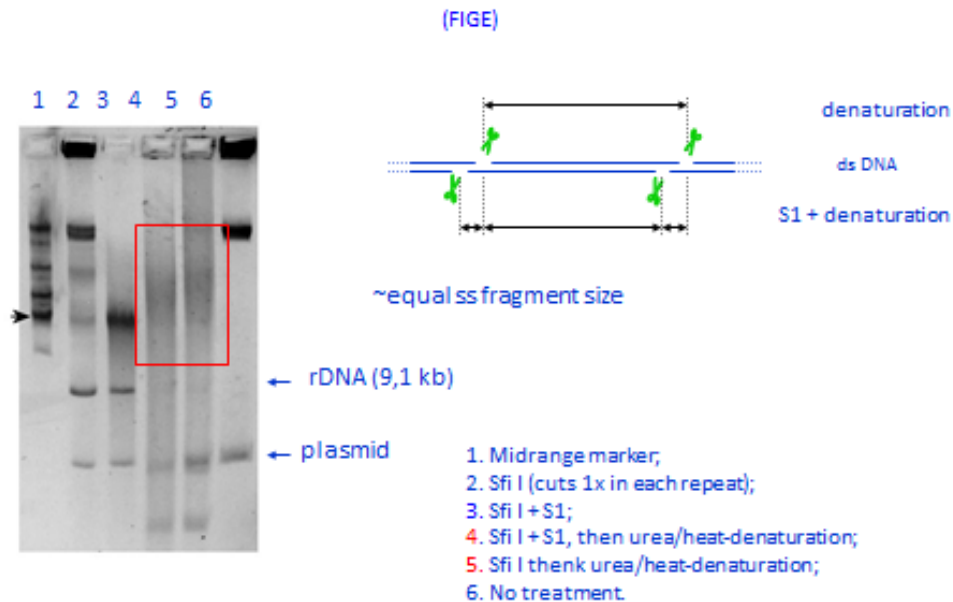


20. The nicks on the opposite strands are arranged in a correlated, staggered arrangement, in the whole genome, in line with what ss-size comparison of rDNA before and after S1 digestion suggested (see #15; above).

### Relationship of ss and ds breaks

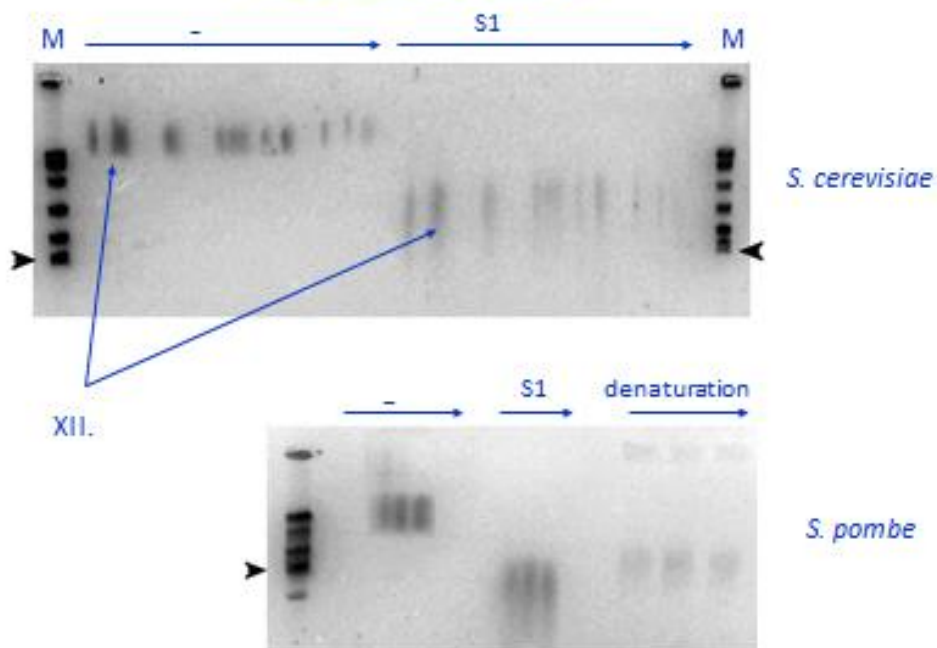


### Relationship of ss and ds breaks



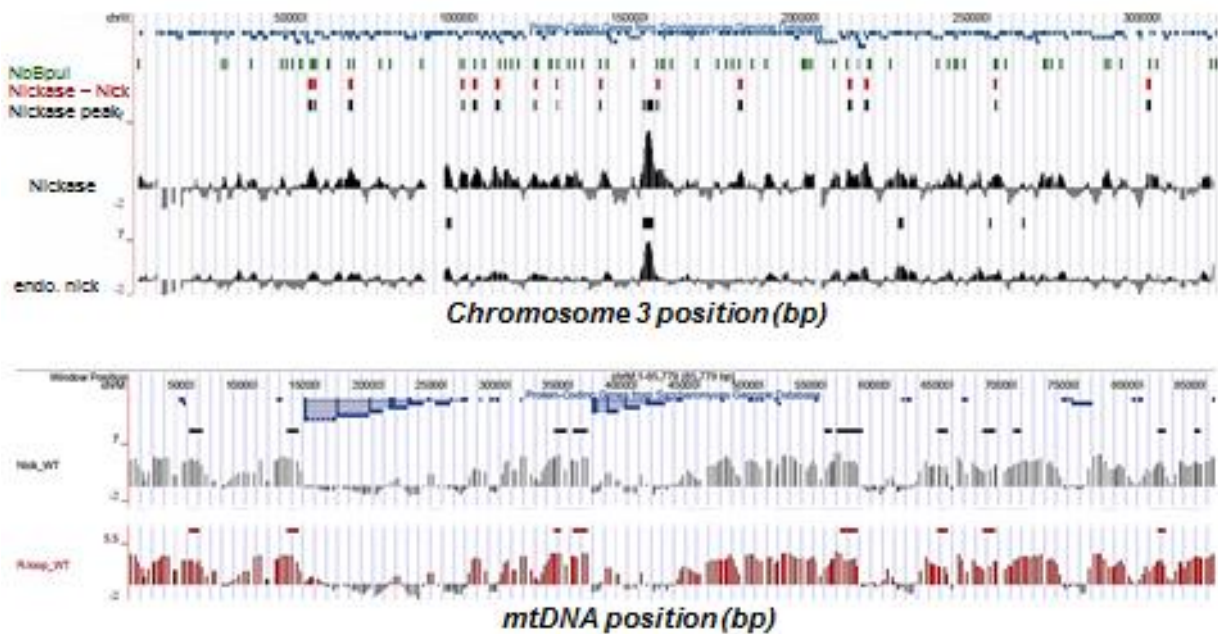
21. The characteristics of the rDNA locus are not exceptional in the *S. cerevisiae* genome, as they appeared to share those of the whole genome, as shown in 2D analysis of the incidence of nicks in the different *S. cerevisiae* (and *S. pombe*) chromosomes. The separated chromosomes were run on denaturing urea-agarose gels or after S1 digestion in neutral agarose gels (see Y dimension). Arrows show at the 50 kb marker.

## Chromosome XII behaves similarly to other chromosomes



22. We have mapped endogenous nicks as well as R-loops on the whole genome level in 3 independent ChIP-on-chip experiments, each time with appropriate input controls, using the above labeling strategies (limited nick-translation; S9.6), on whole genomic tiling arrays (Agilent). The results are in line with a non-random distribution of both entities and are detailed below. Nickase-generated artificial nicks, and the already known nicks and R-loops of the mitochondrial genome served as internal controls.

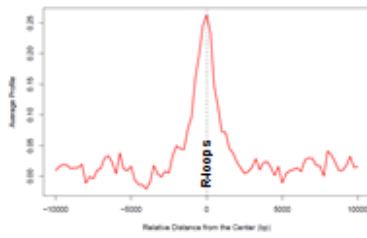
### Chromosomal profiles of R-loops and nicks: **internal controls**



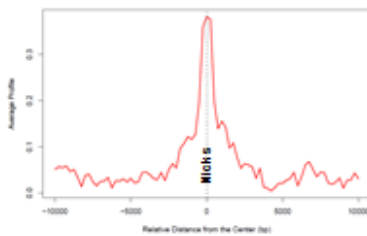


23. Nicks and R-loops coincide to a significant degree, even without the mitochondrial DNA being considered; in the latter case, other reports on their coincidence has been confirmed in our studies. Coincidence has been verified using different bioinformatic approaches, e.g. anchor plots.

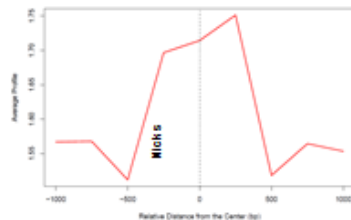
Nick average ChIP profile over R-loops



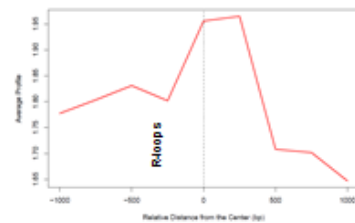
R-loop average ChIP profile over Nicks



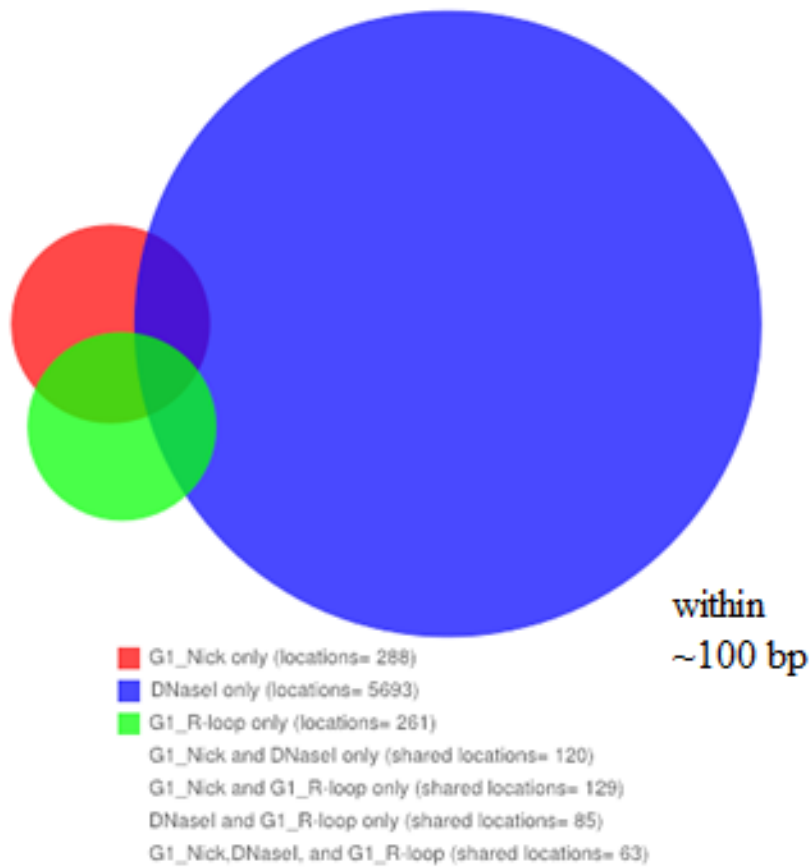
RNAPII average ChIP profile over Nicks



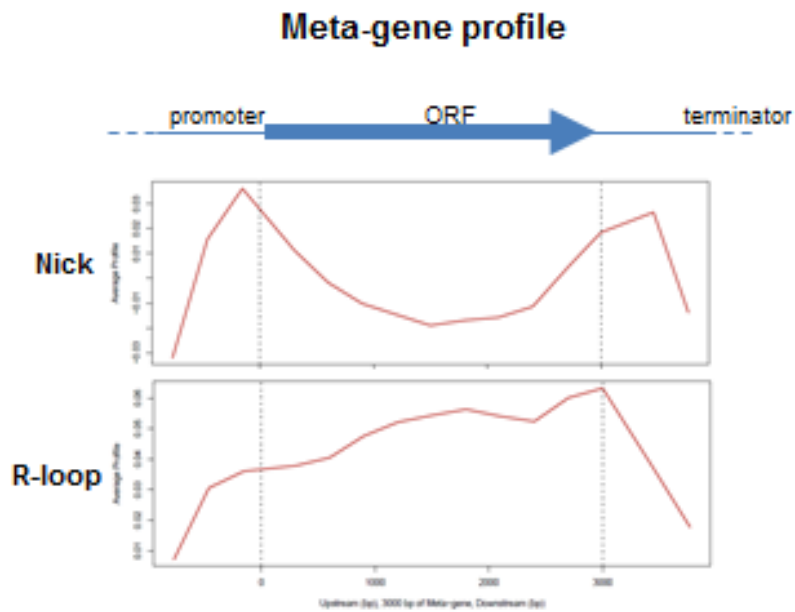
RNAPII average ChIP profile over R-loops



24. Significant coincidence of nicks could be revealed with DNase HS sites and RNA polymerase II occupied sites as well.



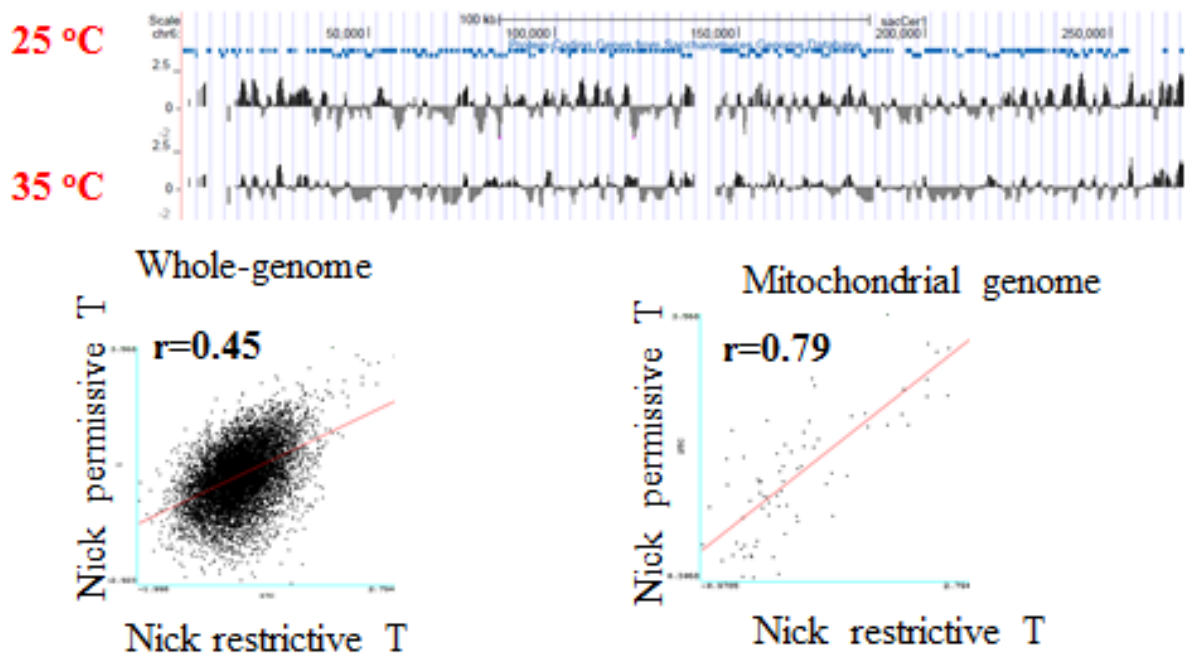
25. Nicks are enriched both around promoters and at around the terminator regions of genes, as revealed in metagene analysis, in this organism that barely has any intergenic region. (Chipseq experiments using human cells have also been conducted, in the framework of Lorant Szekvolgyi's PD OTKA project, with strikingly similar landscapes of these entities within the genes.)



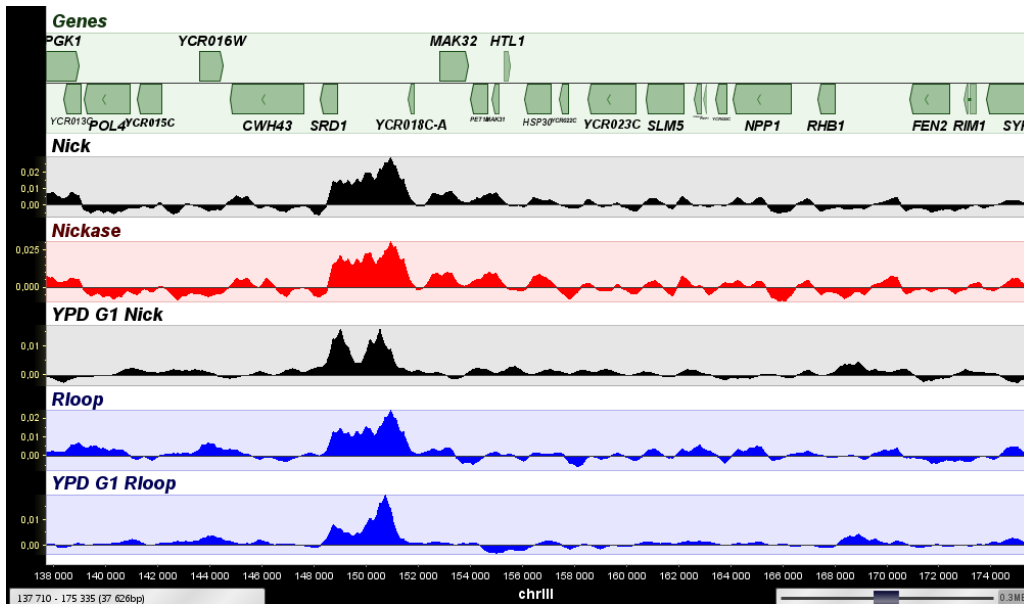
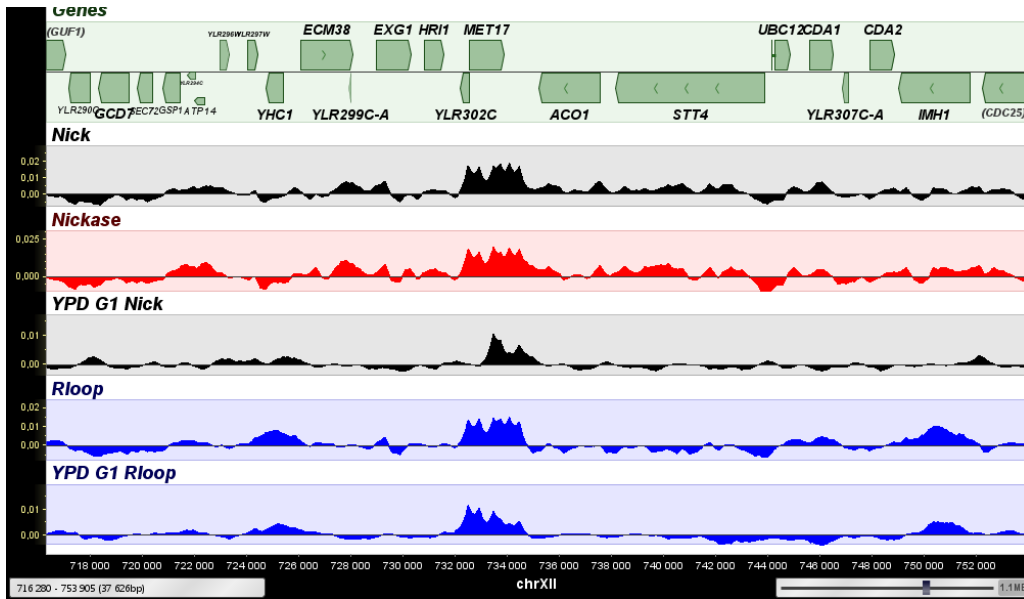
26. The incidence of nicks is dependent on transcription also in *S. cerevisiae* (for mammalian cells see alfa-amanitine effect, above), as shown by the decrease of nick incidence in *rpb5* mutant cells lacking a subunit required by the three RNA polymerases that are functional outside mitochondria.

P39.

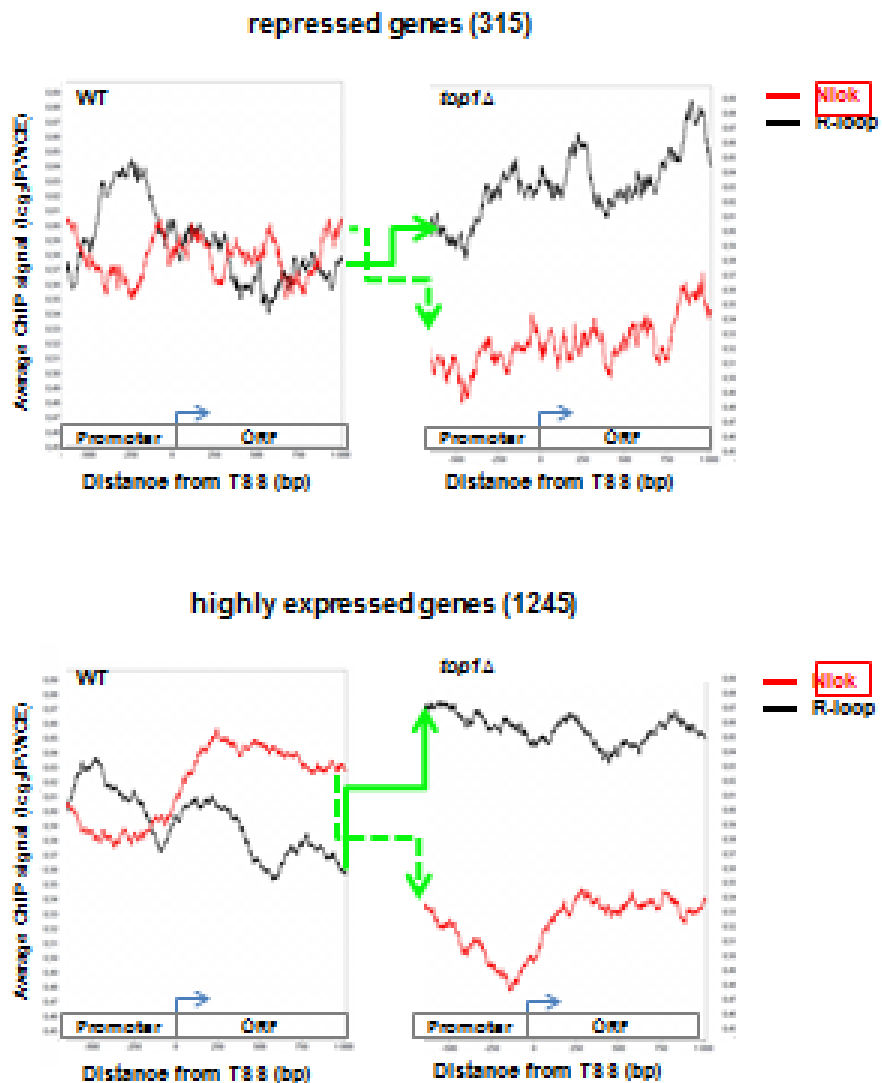
### Chromosomal profile of nicks in an *rpb5-ts* mutant at permissive and restrictive temperatures



27. The replication-independent incidence of nicks, deduced also from earlier data as well as the presence of nicks in G1 phase cells demonstrated in the halo experiments in mammalian cells (see above), was confirmed using alfa-factor synchronized cells (see G1, below), with their altered DNA distribution verified by flow-cytometry (not shown).



28. The incidence of nicks and R-loops appears to be sensitive to various mutations, including *top1*, and metabolic conditions (lactate, galactose, etc. medium; these latter data have been obtained within the framework of Lorant Szekvolgyi's PD OTKA project and are to be discussed in that report). However, the incidence and distribution of nicks detected by nick-translation labeling has not been altered in *Fob1* mutants, i.e. these nicks are not identical to those attributed to the function of the RFB outside the 25S rDNA region where we also see the nicks using the Southern blot approach. (See also 15-17; above.)



## **Summary**

The overall picture emerging from the above results is that the nicks we see genome-wide arise upon transcription, perhaps generated by topoisomerases, in concert with recent reports revealing transient nick-translation/TdT labeling at promoters upon their activation, as well as the presence of topoisomerase II (10-14). Transcription and replication appear to proceed within the „matrix” domain, in accordance with the now prevailing scenario envisioning transcription and replication factories where the DNA reels through, rather than the proteins themselves. The accumulation of nicks and R-loops at the promoter and terminator regions demonstrated in this project fits this picture nicely, with the supercoiled DNA being positioned between anchorage points involved in controlling gene expression. These strategic points are found just under the nuclear lamina, suggesting to identify the enigmatic nuclear matrix as the lamina itself. The very sites of nick/R-loop accumulation must be relaxed regarding superhelicity; the strong and modification specific histone mobilizing effect of an increased twist/writhe ratio argues for an intricate regulation of superhelicity at the border of the two topological domains. The striking correlation between the abundance in R-loops and genomic instability, observed in many systems (15-17), may be explained by the juxtaposed discontinuities revealed and mapped in this project.

## **New methods developed within the framework of the OTKA grant**

Several novel methods have been developed in the course of experimentation. These include a novel gelelectrophoretic technique, a novel rSouth-Western procedure to map R-loops, an LSC-based measurement of loop-size and superhelicity, an LSC-based measurement of histone-DNA affinity and a flow-cytometric microbead assay for detection of varied genetic disorders.

In order to be able to detect nicks, i.e. single-strand discontinuities at a strand-specific manner in the rDNA locus, we were compelled to work out a gelelectrophoretic method that can distinguish two identical size, complementary single-stranded fragments in the 10 kb range (Hegedüs E et al. Separation of 1-23-kb complementary DNA strands by urea-agarose gel electrophoresis. *Nucleic Acids Res.* 2009 Sep;37(17):e112.)

Stemming from our observations on the effect of EBr on DNA melting temperature, a simple, flow-cytometric platform was elaborated and patented for the diagnosis of various genetic conditions. This assay is based on the measurement of fragment length via assessing the melting characteristics of microbead-attached PCR products. (Imre L

et al. Detection of mutations by flow cytometric melting point analysis of PCR products. *Cytometry A*. 2011 Sep;79(9):720-6.)

We have developed an LSC-based assay of various global nuclear parameters (Szekvolgyi L et al. Flow cytometric and laser scanning microscopic approaches in epigenetics research. *Methods Mol Biol*. 2009;567:99-111.), including nucleosome-DNA affinity resolved in a cell cycle phase dependent manner. The latter method has been used to demonstrate that H3K4me3-modified histone containing histone tetramers bind to DNA much weaker than bulk histones or H3K27me3 modified histones. This effect was further analyzed using a panel of antibodies specific to various histone modifications to determine if reader proteins specific to H3K4me3 or co-acetylation on the same nucleosome explain the phenomenon (ongoing studies). The assay system has wide potential applicability for measuring the effect of chromatin interacting drugs, and was patented as a HTP technology serving that purpose. It offers sensitive means to determine, quantitatively and in a cell-cycle phase specific manner, a major component of global histone mobility: nucleosome-DNA cohesion.

We have developed a novel LSC based method to measure loop-size and superhelicity, also in a cell-cycle phase dependent fashion. The method offers means to determine superhelical densities on an absolute scale, fulfilling a goal that has not been reached before, due to our normalization using single-molecule measurements.

### **Indirect impact of the project**

An international conference, the 23rd Wilhelm Bernhard Workshop on the Cell Nucleus was organized by the PI of this project in August, 2013, with many high profile invited speakers (<http://wbw23.unideb.hu/>).

Postdoctoral training of 5 Ph.D. students have been fully or partly accomplished within the framework of this project, yielding one defended Ph.D. thesis (Éva Hegedüs), two others to be submitted within the next half year (László Imre and György Fenyőfalvi) and with two first-year Ph.D. students starting their projects.

### **Publications with OTKA support noted**

see publications in OTKA-EPR

### **Patents (mentioned in the text)**

1. Cytometric method for the comparative analysis of the length of PCR products and uses of this method, PCT/HU2009/000104; 228 175, 2012



2. Imre, L, Szabó G: Quantitative in situ measurement of histone-DNA interaction  
No P1200081, patent, 2012

### **Manuscripts in preparation (1-4)**

Still prevailing uncertainties, to be resolved before submittal of the yet unpublished data to high-profile journals is attempted:

-the effect of top1delta mutation or silencing in MCF7 is not large enough to enable us interpret the presence of nicks as a consequence of that enzymatic activity. Microarray studies on strains with combined top1, top2 conditional mutations and chipseq experiments on another topoisomerase I silenced and control cell pair, with stable karyotype, are underway. The same yeast topoisomerase 1,2 mutant strains have already been compared at their rDNA locus using our rSouth-Western procedure.

-Our assay system developed for the measurement of superhelicity requires minor refinements to make it applicable for the determination of the absolute twist/writhe values. We also plan to compare the early vs. late replicating chromatin in this winding assay to see if euchromatin and heterochromatin differ in halo size and superhelicity, to demonstrate that what the technique measures has functional relevance.

-We are considering to make immuno-electronmicroscopic pictures of the lamina-proximal R-loops.

-The rDNA yeast data are still somewhat controversial regarding the relationship of the nicks observed by us, and the RFB related ones already described. Control experiments using the Southern blot approach are on the way to better clarify this issue.

Some of the above issues are addressed now in collaboration with the Laboratory of Molecular Pharmacology at NIH, making use of a Fulbright fellowship obtained by the PI of this OTKA grant to complete and further develop the topoisomerase related aspects of the current project.

1. Chromatin loops formed by genes are anchored to the periphery of the nucleus via their promoter and terminator regions. (Lorant Szekvolgyi, Andras Szanto, György Fenyőfalvi and Gábor Szabó)

2. Histone tetramer – DNA binding affinity is highly sensitive to certain posttranslational modifications and superhelical stress. (László Imre, Zoltán Simándi, László Nagy, Hiroshi Kimura and Gábor Szabó)

3. Measurement of the size and superhelical density distribution of chromatin loops in nuclear halos by laser scanning cytometry. (György Fenyőfalvi and Gábor Szabó)

4. Global mapping of endogeneous nicks and R-loops in HCHO-fixed *S. cerevisiae*. (Lóránt Szekvolgyi, Éva Hegedüs, András Szántó and Gábor Szabó)

5. Mapping of nicks and R-loops at the rDNA locus of *S. cerevisiae*. (Éva Hegedüs, Lóránt Szekvolgyi, Endre Kókai, Viktor Dombrádi, Aziz el Hage and Gábor Szabó)

## References

1: Szekvolgyi L, Rákosy Z, Bálint BL, Kókai E, Imre L, Vereb G, Bacsó Z, Goda K, Varga S, Balázs M, Dombrádi V, Nagy L, Szabó G. Ribonucleoprotein-masked nicks at 50-kbp intervals in the eukaryotic genomic DNA. *Proc Natl Acad Sci U S A*. 2007 Sep 18;104(38):14964-9.

2: Szilágyi I, Varga T, Szekvolgyi L, Hegedüs E, Goda K, Kaczur V, Bacsó Z, Nakayama Y, Pósaí J, Pongor S, Szabó G Jr. Non-random features of loop-size chromatin fragmentation. *J Cell Biochem*. 2003 Aug 15;89(6):1193-205.

3: Gál I, Varga T, Szilágyi I, Balázs M, Schlamadinger J, Szabó G Jr. Protease-elicited TUNEL positivity of non-apoptotic fixed cells. *J Histochem Cytochem*. 2000 Jul;48(7):963-70.

4: Varga T, Szilágyi I, Szabó G Jr. Single-strand breaks in agarose-embedded chromatin of nonapoptotic cells. *Biochem Biophys Res Commun*. 1999 Oct 22;264(2):388-94.

5: Szabó G Jr, Bacsó Z. Chromatin isolated from viable human PBLs contains DNA fragmented to  $\geq 50$  kb. *Cell Death Differ*. 1996 Apr;3(2):237-41.

6: Szabó G Jr, Boldog F, Wikonkál N. Disassembly of chromatin into approximately equal to 50 kb units by detergent. *Biochem Biophys Res Commun*. 1990 Jun 15;169(2):706-12.

7: Szabó G Jr. 50-kb chromatin fragmentation in the absence of apoptosis. *Exp Cell Res*. 1995 Dec;221(2):320-5.

8: Kim N, Huang SN, Williams JS, Li YC, Clark AB, Cho JE, Kunkel TA, Pommier Y, Jinks-Robertson S. Mutagenic processing of ribonucleotides in DNA by yeast topoisomerase I. *Science*. 2011 Jun 24;332(6037):1561-4.

9: Sordet O, Nakamura AJ, Redon CE, Pommier Y. DNA double-strand breaks and ATM activation by transcription-blocking DNA lesions. *Cell Cycle*. 2010 Jan 15;9(2):274-8.

- 10: Li X, Niu T, Manley JL. The RNA binding protein RNPS1 alleviates ASF/SF2 depletion-induced genomic instability. *RNA*. 2007 Dec;13(12):2108-15.
- 11: Haffner MC, De Marzo AM, Meeker AK, Nelson WG, Yegnasubramanian S. Transcription-induced DNA double strand breaks: both oncogenic force and potential therapeutic target? *Clin Cancer Res*. 2011 Jun 15;17(12):3858-64.
- 12: Androgen-induced TOP2B-mediated double-strand breaks and prostate cancer gene rearrangements. *Nat Genet* 2010;42:668–75.
- 13: DNA oxidation as triggered by H3K9me2 demethylation drives estrogen-induced gene expression. *Science* 2008;319:202–6.
- 14: A role of DNA-PK for the metabolic gene regulation in response to insulin. *Cell* 2009;136:1056–72.
- 15: Bochkareva A et al. Factor-independent transcription pausing caused by recognition of the RNA-DNA hybrid sequence. *EMBO J*. 2011 Nov 29.
- 16: Gan W et al. R-loop-mediated genomic instability is caused by impairment of replication fork progression. *Genes Dev*. 2011 Oct 1;25(19):2041-56.
- 17: Gómez-González B et al. Genome-wide function of THO/TREX in active genes prevents R-loop-dependent replication obstacles. *EMBO J*. 2011 Jun 24;30(15):3106-19.